Available online at www.sciencedirect.com

ScienceDirect

Proceedings of the Combustion Institute 39 (2023) 179–188

Proceedings of the Combustion Institute

www.elsevier.com/locate/proci

Towards a predictive kinetic model of 3-ethyltoluene: Evidence concerning fuel-specific intermediates in the flow reactor pyrolysis with insights into model implications

Qianpeng Wang [a], Mo Yang [a], Juan Wang [a,*], Jiuzhong Yang [b,*], Long Zhao [b], Wang Li [b], Changyang Wang [b], Tenglong Lu [b], Yujun Li [c]

[a] *National Key Laboratory of Science and Technology on Aero-Engine Aero-Thermodynamics, School of Energy and Power Engineering, Beihang University, Beijing 100191, PR China*

[b] *National Synchrotron Radiation Laboratory, University of Science and Technology of China, Hefei, Anhui 230029, PR China*

[c] *State Key Laboratory of High Temperature Gas Dynamics, Chinese Academy of Sciences, Beijing 100190, PR China*

Received 5 January 2022; accepted 18 July 2022
Available online 22 September 2022

Abstract

To reveal insights into high temperature kinetics of dialkylaromatics, a pyrolysis investigation of 3-ethyltoluene in a flow reactor together with its reaction kinetics are presented in this work. Concentrations and chemical structures of specific species covering temperature range from 796 to 1383K at the pressure of 30 and 760 Torr were recorded and quantified by using synchrotron vacuum ultraviolet photoionization molecular-beam mass spectrometry (VUV-PI-MBMS). Important C_8 and C_9 fuel-specific intermediates relevant to primary decomposition of 3-ethyltoluene and isomerization of methylbenzyl and ethylbenzyl radicals were detected and identified. The kinetic model interpreting high temperature pyrolysis chemistry of 3-ethyltoluene was developed and reasonably predicted the measurements in this work. The model analyses reveal that the methyl-dissociated reaction from the ethyl group of 3-ethyltoluene is dominant in the fuel decomposition at low pressure, while the fuel is mainly consumed by hydrogen abstraction reactions at atmospheric pressure. The experimental observations of three methylbenzyl isomers, *o*-xylylene, *p*-xylylene, styrene and benzocyclobutene provide evidence for the relationships between products involving isomerization of methylbenzyl radicals, formation of xylylenes and decomposition of *o*-xylylene. The fuel structure effects of 3-ethyltoluene and *m*-xylene are revealed by comparing the pyrolysis behaviors in both cases. It has been found that the *m*-methylbenzyl-generating channel in the 3-ethyltoluene pyrolysis improved the reac-

* Corresponding author.
E-mail addresses: juanwang@buaa.edu.cn (J. Wang), jzhyang@ustc.edu.cn (J. Yang).

https://doi.org/10.1016/j.proci.2022.07.150

tion reactivity initially. Furthermore, the fuel with longer substituent ethyl group facilitates the formation of cycloalkenes and aromatics.

Keywords: 3-Ethyltoluene; High temperature pyrolysis; Aromatics; Kinetic modeling; Methylbenzyl radical

1. Introduction

Hazardous emissions from incomplete combustion of fossil fuels, such as polycyclic aromatic hydrocarbons (PAHs) and soot matters, adversely affect human health and air quality. Challenges and puzzles remain in uncovering the PAH and soot formation mechanism in complicated combustion systems. Most combustion kinetics of aromatic fuels in the literature focused on the monoalkylbenzenes [1,2] through experimental observations and numerical techniques under various conditions. The roles of polyalkylbenzenes on PAHs and soot growth under combustion still need to be revealed. Hemelsoet et al. [3] reported that the methyl substituent enhanced the coke formation of methylated aromatics during thermal cracking with hydrogen abstractions. Based on this perspective, further considerations for the substitution effect of dialkylated aromatics on the fuel decomposition and PAH growth are required. Several experimental endeavors have been conducted to describe the combustion or oxidation of xylenes ($C_6H_4(CH_3)_2$), involving global combustion characteristics, such as flame propagations [4,5] and ignition properties [6,7], and speciation measurements [8–11]. With regard to experimental and chemical details of ethyltoluenes, the only measurement of ignition delay time was reported for *o*-ethyltoluene in a rapid compression machine [12]. In addition, 3-ethyltoluene is the major component of aromatics chemical class in practical and surrogate kerosene fuels [13]. Thus, it is indispensable and fundamental to reveal the combustion chemistry of 3-ethyltoluene based on detailed experimental detection of a large variety of intermediates.

Since the kinetic parameters of decomposition reactions for fuel-specific radicals are critical for fuel consumption in numerical simulations, many experimental and theoretical efforts have been made to verify the isomerization pathways of *o*-, *m*- and *p*-methylbenzyls in individual combustion systems. With high-resolution MBMS [11,14,15] and high-level theoretical investigations [16], the decomposition patterns of *o*- and *p*-methylbenzyls to *o*- and *p*-xylylenes, and mutual isomerizations of three methylbenzyl radicals were gradually established. However, to improve the understanding in the mechanism of methylbenzyl isomerizations, the evidence of *m*-methylbenzyl isomerizing to *o*- and *p*-methylbenzyls deserves more theoretical derivations and experimental explorations. The rearrangements of *m*-methylbenzyl and *m*-ethylbenzyl relevant to predictive aromatic model still need a clear kinetic description. The first target of the present work is to provide speciation datasets of 3-ethyltoluene pyrolysis in a flow reactor with synchrotron vacuum ultraviolet photoionization molecular-beam mass spectrometry (VUV-PI-MBMS) [17]. The second target is to develop a predictive kinetic model for 3-ethyltoluene to interpret the fuel decomposition mechanism and formation of different ethylbenzyls, methylbenzyls, benzocyclobutene, indane and aromatic products. Model implications regarding fuel-specific species as well as their formation pathways are also addressed with combination of experimental observations and kinetic analyses.

2. Experimental approach

The experimental platform for pyrolysis of 3-ethyltoluene is similar to our previous work [18,19]. The configuration of the pyrolysis apparatus has been described in detail by Qi [17], and thus only the updates are provided below. The experimental apparatus is consisted of a flow reactor, a differentially chamber, and a photoionization system. In the present work, the pressure of the flow tube was controlled at 30 or 760 Torr, and the gas flow rates of the fuel and diluent gases (krypton and argon) were kept at 2.5, 5 and 992.5 standard cubic centimeters (SCCM), respectively. To obtain a broader isothermal region of high temperature, the heated length of the flow tube was extended to 400 mm. Regarding the identification of pyrolytic species, the photoionization efficiency (PIE) spectra were used to determine the specific molecule structure by comparing them with the photoionization cross section (PICS) from the corresponding literature. To calculate the mole fraction of each species, we measured the mass spectrum signals under each temperature condition and quantified them following the equations in [17]. The uncertainties of species concentrations are estimated within ±10%, ±20% and a factor of 2 for major species, intermediates and species with estimated PICSs [17], respectively.

3. Kinetic model development

The depletion mechanisms of 3-ethyltoluene were partly explored in the *m*-xylene models in the literature, including Battin-Leclerc's model [7], Dagaut's model [8], Gudiyella's model [9], Mouis's model [20] and LLNL model [21]. The experimental data in this work was used to verify the kinetic compatibility of these *m*-xylene models. Fig. S1 exhibits the comparison of 3-ethyltoluene concentrations of measured and simulation results by using the above models under the investigated conditions. There is a great discrepancy between the experimental data and predictions employing the above models. Thus, a predictive kinetic model for 3-ethyltoluene is in demand to reveal the reaction pattern for dialkylaromatics. Considering the simulations of the five models at the entire experimental conditions, Battin-Leclerc's model [7], providing a better performance in predicting mole fractions of 3-ethyltoluene compared with the others, is employed as the base model for the development of the kinetic model for describing the high-temperature pyrolysis chemistry of 3-ethyltoluene in this work.

Comparing with the stable characteristics of benzene ring, the reaction mechanisms related to the methyl and ethyl substitutes are the main kinetic work of 3-ethyltoluene. In the initiation reactions, rate coefficients derived from the ethylbenzene study [2] were integrated into the current model for the C−C bond scission reactions of the ethyl group. And the methyl group scission channel followed the rate rules in Battin-Leclerc's model [7] with a half shift of modification considering the moiety substituent of *m*-xylene. For the C−H bond scission reactions, the pressure-dependent rate constants from an early recommendation by Mizerka and Kiefer [22] were adopted in the current model. In view of the structure feature of 3-ethyltoluene, monocyclic aromatic products like toluene, *m*-xylene and ethylbenzene mainly originate from ipso-substitution reactions by H-atom on both ethyl and methyl side chains. The rate coefficients for these ipso-substitution pathways derived from the toluene study ranging from 873 to 923 K were used in Battin-Leclerc's model [7]. However, in the present model for *m*-xylene and ethylbenzene formation, these ipso-substitution reactions were updated from an ethylbenzene study aiming at high temperature combustion by Ergut et al. [23].

The hydrogen abstraction reactions have been proven as the important type of reactions contributing to the decomposition of aromatic fuels [24]. Thus, the hydrogen abstractions taking place at phenylic, benzylic, primary and secondary phenethylic positions should be thoroughly considered. In this work, theoretical calculations on the C−H bond dissociation energies (BDEs) of each side chain were conducted at CBS-QB3 level. Based on the calculated energies and molecular properties, the rate constants of these reactions were assigned from the similar reactions of *m*-xylene [7]. The reaction pathways of the fuel radicals, including methylethylphenyl ($CH_3C_6H_3C_2H_5$), ethylbenzyl ($\dot{C}H_2C_6H_4C_2H_5$), 1-tolylethyl ($CH_3C_6H_4\dot{C}HCH_3$) and 2-tolylethyl ($CH_3C_6H_4CH_2\dot{C}H_2$), were included in the present work, and the corresponding rate coefficients were mainly taken from the work of [7] or estimated by analogy with the similar reactions of toluene [25] and ethylbenzene [2].

Particular attention should be paid to *o*-methylbenzyl radicals that can generate benzocyclobutene and styrene [15]. The experimental observations in this work provided the evidence of these products. Thus, the formation pathways of benzocyclobutene and styrene from *o*-methylbenzyl, as well as indane and 2-propenylbenzene from ortho C_9H_{11} fuel-specific radicals, were integrated into the current kinetic model. The rate coefficients for the isomerizations of *o*-methylbenzyl, *o*-ethylbenzyl and tolylethyl radicals were determined considering the concentrations of benzocyclobutene, styrene and indane from the present experimental results. Specifically, for the isomerization reactions of *m*-methylbenzyl to *o*- and *p*-methylbenzyl radicals, the rate parameters for these two reactions were introduced into the present model from a recent *o*-xylene oxidation work [26]. For the decomposition of *o*- and *p*-methylbenzyl to *o*- and *p*-xylylene plus H, model performances have been tested by using two sets of kinetic parameters from theoretical results [16] and shock tube measurements [27]. However, the studies of Fernandes et al. [27] were conducted at high pressures up to 4 bar, which may be inharmonious to the present investigated conditions (0.04 and 1 atm). Thus in the present work, considering the need of pressure-dependent rate coefficients for the decomposition of *o*- and *p*-methylbenzyl radicals, we follow the rules from the up to date kinetic results (da Silva's paper [16]) with a reduction to the reasonable values compared with Fernandes's study [27]. It should be noted that the measured concentrations of *o*-xylylene and *p*-xylylene were taken as the criterion role in the optimization of rate constants for these two reactions. Regarding the decomposition of *o*-xylylene and further transformation of benzocyclobutene to styrene, the experimental results for benzocyclobutene and styrene play the role of benchmarking in the rate confirmation from Battin-Leclerc's model [7]. And for the determination of the rate coefficients for the isomerizations of *o*-ethylbenzyl and tolylethyl radicals, we follow the rules in the isomerization pathways of methylbenzyl radicals in the work of da Silva et al. [16]. Simulations in this work were performed using the plug flow reactor (PFR) module in ANSYS Chemkin-Pro 19.2. Input parameters including reactor di-

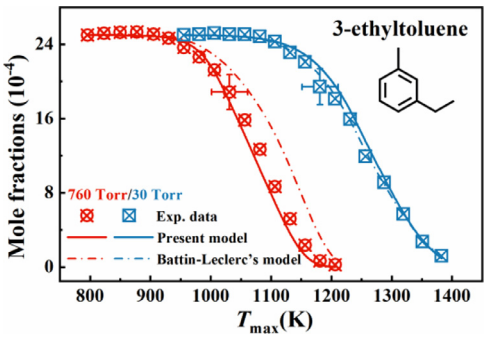

Fig. 1. Measured (symbols) and simulated (lines) fuel concentration profiles as a function of T_{max} in the pyrolysis of 3-ethyltoluene. Solid and dash dot lines denote simulations using the current and Battin-Leclerc's model [7].

mensions, volumetric flow rates and measured axial temperature profiles were introduced under different conditions. The measured temperature profiles together with the kinetic model and thermochemical data are available in the *Supplementary Material*.

4. Results and discussion

4.1. Primary decomposition of the fuel

In this work, over thirty intermediate species were detected and identified in the pyrolysis of 3-ethyltoluene, including C_1–C_6 low molecular weight species, monocyclic and polycyclic aromatics. The experimental fuel concentration profiles and simulation results from the current model and Battin-Leclerc's model are illustrated in Fig. 1. It is found that both models can well simulate the fuel reactivity at 30 Torr. As for the simulation comparison at atmospheric pressure, the variation tendency of fuel depletion is precisely calculated by the current kinetic model, whereas it is overpredicted by the Battin-Leclerc's model. Notable improvements have been achieved by the current model in predicting the kinetics of fuel consumption.

In order to reveal the chemical pathways for the fuel decomposition, the rate of production (ROP) and sensitivity analyses were performed at nearly 30 Torr, 1257 K and 760 Torr, 1081 K, respectively to enable the reaction process reach around 50% fuel conversion. As shown in Fig. 2a, the unimolecular dissociation reaction to produce *m*-methylbenzyl and methyl radicals (reaction R1) takes a dominant role in decomposing 3-ethyltoluene with a fuel depletion ratio of about 27% at 760 Torr and even more than half of the fuel at 30 Torr. The ethyl-dissociated reaction R2 also exhibits relatively strong reactivity in the fuel decomposition at 30 Torr. However, R2 at atmospheric condition and the C−C dissociation reaction R3 merely present the minor contributions to the fuel consumption. The sensitivity analysis of 3-ethyltoluene shown in Fig. 2b also delineates the similar results that the unimolecular dissociation reaction on ethyl side chain exhibits strong sensitivities for 3-ethyltoluene, and the unimolecular dissociation on methyl side chain (reaction R3) only has a low sensitivity. Furthermore, theoretical calculations of BDEs of C−C and C−H bonds on the side chain of 3-ethyltoluene were conducted based on the CBS-QB3 method with the geometry optimization at B3LYP/CBSB7 level and the results are shown in Fig. S2 of the *Supplementary Material*. Compared with BDEs for reactions R2 and R3, methyl-dissociated reaction R1 owns the lowest BDE about 78.7 kcal/mol among reactions via C−C rupture. The dominant fuel consumption pathway and strong sensitivities for the fuel can be partly rationalized by the fact that the lower BDEs of C−C bond on the ethyl side chain facilitate the fuel decomposition at a higher reactivity.

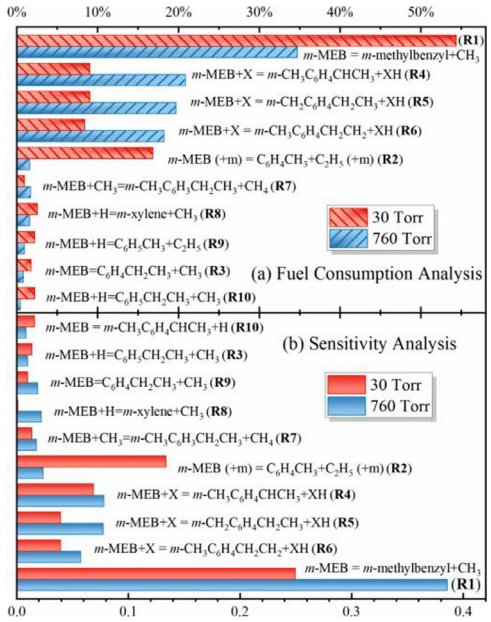

Fig. 2. Results of (a) percentage contributions of major fuel consumption pathways and (b) sensitivity analysis of fuel from the current model at 30 Torr, 1257 K and 760 Torr, 1081 K. *m*-MEB (*m*-methylethylbenzene) denotes 3-ethyltoluene. X and XH denote the sum of radical reactants and reaction products for hydrogen abstractions.

On the other hand, the fuel consumption of the hydrogen abstraction reaction occurs along with that of unimolecular channels. Fig. 2a depicts the percentage consumptions of hydrogen abstraction reactions at different carbon sites, producing three types of side-chain fuel radicals namely 1-tolylethyl, *m*-ethylbenzyl and 2-tolylethyl radicals

(reactions R4, R5 and R6). Detailed structures for these fuel radicals with their formulas and nomenclatures can be found in the *Supplementary Material*. The maximal differential value for C−H bond energy is nearly 13.9 kcal/mol, which is half of that for C−C bonds of R1 and R3 (nearly 27.4 kcal/mol) as shown in Fig. S2. Therefore, thermodynamics properties play an important role in initial reactions of the fuel pyrolysis system. Among the fuel consumption pathways via hydrogen abstractions, reaction on the secondary C−H site (R4) of ethyl side chain is favored due to the weak bond energy with a percentage contribution about 27% at 760 Torr and decreasing to around 7% at low pressure. Similarly, lower decomposition reactivity with the decrease of pressure occurring on the reactions R5 and R6 reveals that the reaction pathways of the fuel consumptions are not only attributed to the thermodynamics properties, but also to the pressure-dependent kinetics. Regarding the directly hydrogen abstraction from the aromatic ring, negligible contribution provided by R7 to the fuel decomposition indicates that this reaction is unfavorable under the combustion-related conditions of the fuel. Furthermore, sensitivity analyses in Fig. 2b also endorse this point that reactions R4−R7 become more influential to the decomposition reactivity of 3-ethyltoluene with pressure rising. Ipso-substitution reactions were actually considered as the typical pathways in kinetic study of diverse aromatics [2,24,28]. In this study, substituents in 3-ethyltoluene can be replaced by H atom to form toluene, *m*-xylene and ethylbenzene. Particularly, high concentrations of toluene and *m*-xylene detected in this study benefit from these initial pathways, although each of them consumes fuel no more than 3%. This observation is in accordance with those in the pyrolysis studies of ethylbenzene [2] and *tert*-butylbenzene [28].

According to the above discussion, the high contributions and sensitivity of methylic C−C bond fission on ethyl group (R1) and hydrogen abstraction reactions on each side chain (R4, R5 and R6) indicate the vital role of initial reactions in the fuel consumption. Furthermore, initiation pathways of ipso-substitution also present significant influences on the fuel consumption and chain reactions of alkylaromatics. Therefore, it is noteworthy to improve the accuracy of model prediction with the consideration of important channels and their corresponding pressure-dependent kinetic parameters in the present work.

4.2. Isomerization of C_8 and C_9 fuel-specific intermediates

Varied fuel-specific intermediates are generated from the primary decomposition process, including high concentrations of *m*-methylbenzyl, *m*-ethylbenzyl, 1-tolylethyl and 2-tolylethyl radicals. The kinetic analysis of *m*-methylbenzyl has revealed that the main termination of *m*-methylbenzyl is to transform to ortho and para radical isomers, which can further decompose to closed-shell *o*-xylylene and *p*-xylylene [14–16]. The rearrangements of the three methylbenzyl radicals have also been inferred by the experimental observations that *p*-xylylene serves as a decomposition product in the pyrolysis of *m*- and *o*-methylbenzyl radicals [14,15]. However, the mechanism for describing the isomerization and decomposition of three methylbenzyl isomers is still lacking in the literature. The missing of *m*-methylbenzyl reactions in mechanism of *m*-xylene flame [11] resulted in the overestimation of the fuel radicals. This indicates that degradation channels of *m*-methylbenzyl should be carefully considered in initial decomposition of xylenes.

In the current work, the identification of methylbenzyl isomers ($m/z = 105$) is presented in Fig. 3a, where the reference ionization energies (IEs) are from the measured results in [15]. Since the IEs for methylbenzyl isomers are in the range from 6.9 to 7.2 eV, partially enlarged view of the PIE spectrum for $m/z = 105$ is displayed here, while the full range (6.9−10.5 eV) PIE spectrum is provided in Fig. S3 of *Supplemental material*. As can be seen from Fig. 3a, three methylbenzyl isomers are observed and distinguished with their respective IEs. The onsets of 6.93 and 6.99 eV are in accordance with the IEs of para and ortho methylbenzyl radicals that indicates the existence of the isomerization of *m*-methylbenzyl to the other two isomers. Furthermore, the curve of linear fitting for m/z=105 shown in Fig. S4 also indicates the presence and distribution of three methylbenzyl radicals. It is noted that both *p*- and *o*-methylbenzyl have relatively low signals compared with the dominate reaction product *m*-methylbenzyl. The formations of *p*- and *o*-xylylene are closely related to the hydrogen-scission reactions of *p*- and *o*-methylbenzyl radicals [15]. The PIE curves for the two xylylenes are provided in Fig. 3b, where two onsets of 7.74 and 7.89 eV correspond to the reference IEs of *o*-xylylene and *p*-xylylene. The experimental and modeling results of xylylene isomers are shown in Fig. 4a and b. The concentration profiles of the two xylylenes share similarity that they have higher mole fractions at 30 Torr than those at 760 Torr, which is attributed to the more stable characteristic at low pressure [14]. The *p*-xylylene formation route has been speculated in [15] via *o*- → *m*- → *p*-methylbenzyl. The channel of *m*-methylbenzyl to *p*-methylbenzyl and then *p*-xylylene was applied in the present work. However, it is less competitive for the isomerization of *o*- to *m*-methylbenzyl in the pyrolysis of 3-ethlytoluene. And *o*-methylbenzyl radicals are more likely to rearrange to benzocyclobutene, which is a typical evidence of existence of *o*-methylbenzyl in *m*-xylene flame [11]. Thus, this pathway was adopted in the present *m*-xylene sub-mechanism and the model simulations of ben-

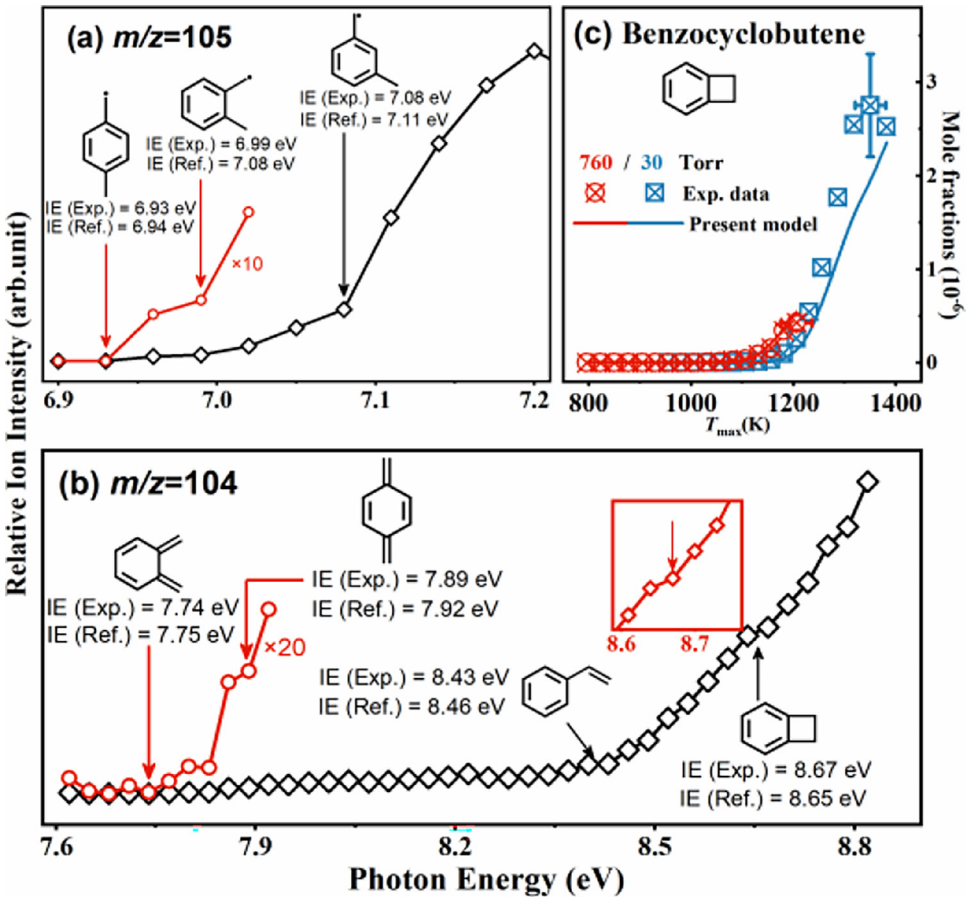

Fig. 3. The measured PIE curves for (a) $m/z = 105$, (b) $m/z = 104$, and (c) the comparison of benzocyclobutene concentration between experimental and modeling results from the pyrolysis of 3-ethyltoluene.

zocyclobutene compared with experimental results are exhibited in Fig. 3c. Another typical evidence for existence of *o*-methylbenzyl is the detection of styrene, which is observed at the obvious onset of 8.43 eV. As mentioned above, the bond fissions can lead to the formation of *o*- and *p*-xylylene. Meanwhile, such reactions dominate the yield of styrene from the C_4 ring-opening of benzocyclobutene as shown in Fig. 4d. With regard to the consumption of styrene, 1-phenyl-1-vinyl ($C_6H_5CCH_2$) and 2-phenyl-1-vinyl (C_6H_5CHCH) radicals are mainly produced through the hydrogen abstractions and further form phenylacetylene with additional hydrogen fission reactions. With including the isomerization of the three methylbenzyl radicals and the transformation from *o*-methylbenzyl to benzocyclobutene and then styrene, the better predictions of styrene and phenylacetylene were achieved to capture the variation of species concentrations as shown in Figs. 4c and S5.

To identify the nine various C_9H_{11} radicals with electronic sites at different substituents in different steric hindrance relations, ionization energies of these intermediates were calculated with the theoretical method of CBS-QB3 as shown in Table S3 with the formulas, nomenclatures and structures for ortho, meta and para radials. Fig. 5a displays the PIE spectrum for $m/z = 119$, where the onsets at 6.93, 7.05 and 7.11 eV are in accordance with the calculated IEs of *p*-, *o*- and *m*-ethylbenzyl, respectively. These experimental observations provide the direct evidences of the existences of ortho and para ethylbenzyl isomers, which also indicate the relevant channels of *p*- and *o*-ethylbenzyl should be considered in a predictive combustion model. The simulations of 3-ethytoluene by Battin-Leclerc's and Dagaut's models [7,8] in Fig. S1 and their ROP analyses in Fig. S6 highlight the importance of C_9 fuel-specific radicals in the pyrolysis of 3-ethytoluene, especially for meta 1-tolylethyl, which contributes over 10% to the fuel consumption through hydrogen abstraction reactions.

As mentioned above, xylylenes can be formed through hydrogen-scission from ortho and para

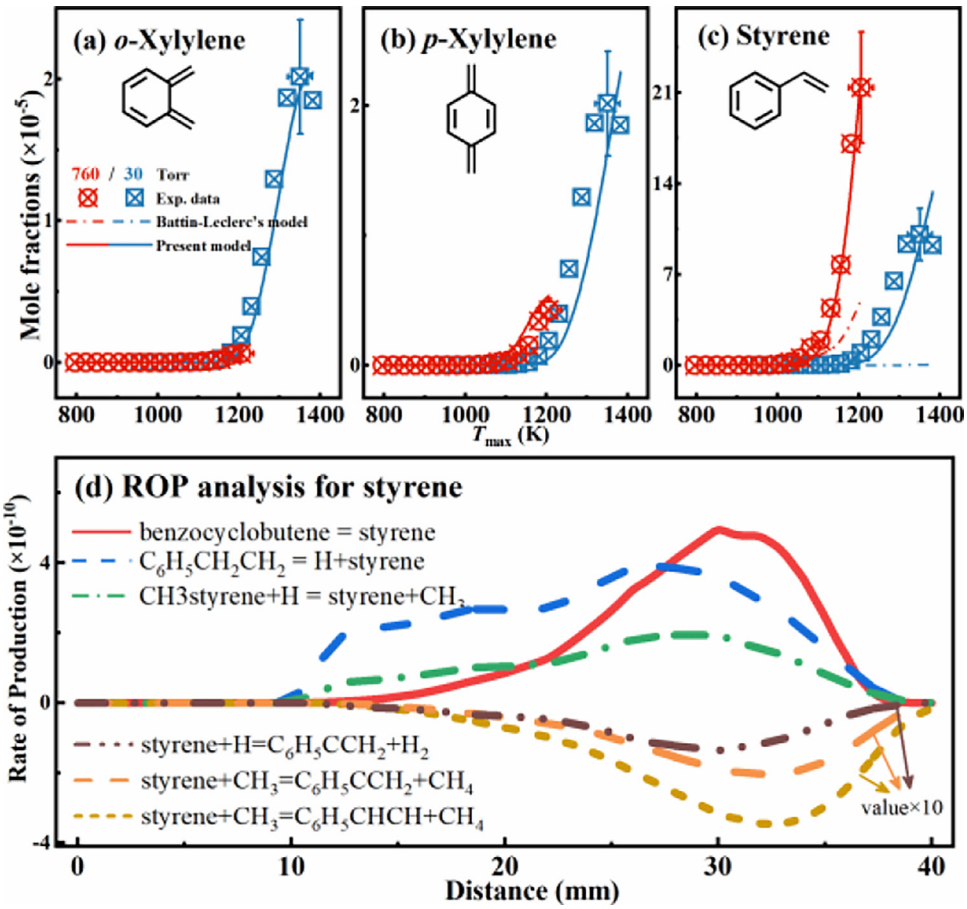

Fig. 4. Comparisons of (a) *o*-xylylene, (b) *p*-xylylene and (c) styrene between experimental and modeling results, and (d) distance-dependent ROP analysis for styrene at about 30 Torr, 1257 K in the pyrolysis of 3-ethyltoluene.

methylbenzyl radicals. And ethylbenzyl radicals can follow the similar decomposition pattern that decompose to closed-shell structure of ortho and para C_9H_{10} products, whose ionization energies are hard to identify at 8.25 eV in Fig. 5b. However, we observed that a slight upwarp at 8.54 eV is in consistency with the literature value of indane, and this evidence confirmed that *m*-ethylbenzyl isomerizes to *o*-ethylbenzyl radical in the pyrolysis of 3-ethyltoluene. This reaction sequence is closely related to the stage of initial fuel decomposition that the produced fuel radicals isomerize to orthotopic isomers and then decompose to indane. The concentration of indane is highly influenced by the bottom reaction sequence shown in Fig. S7. Indane concentrations (not shown) in the modeling results are apparently lower than those from the measurements, and this underestimation can be explained that the signals for indane are obtained without subtracting the section of various C_9H_{10} isomers. At this point, it suggests that it is necessary to identify those signals in further investigations. In contrast, reaction model may be impervious to such deficiency because warranted kinetic analyses with detailed attention have been used to identify targeted products and influential reactions through the complicated reaction network.

4.3. Effects of fuel molecular structure on formation of cycloalkenes and aromatics

Since the fuel molecule 3-ethyltoluene contains a benzene ring, cycloalkenes and aromatics with monocyclic and polycyclic benzene ring are expected to be produced in high reactivity from the pyrolysis of 3-ethyltoluene. Fig. 6 presents the concentrations of cycloalkenes and aromatics products from the measurements and simulations by the current 3-ethyltoluene kinetic model, together with the simulated results of the *m*-xylene pyrolysis from Battin-Leclerc's model [7]. As shown in Fig. 6, the product distributions have noticeable similarities between 3-ethyltoluene and *m*-xylene pyrolysis because *m*-methylbenzyl-

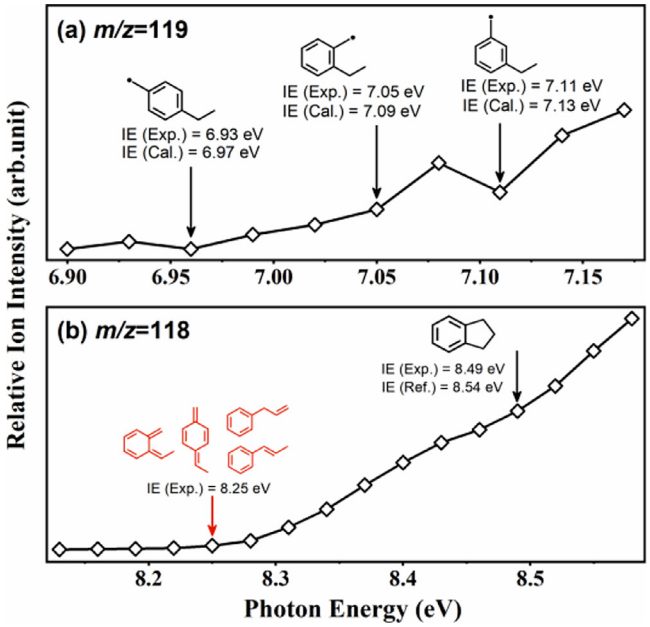

Fig. 5. The measured PIE curves for (a) $m/z = 119$ and (b) $m/z = 118$ from the pyrolysis of 3-ethyltoluene.

generating channel dominates the primary decomposition in both cases. However, the pyrolysis of 3-ethyltoluene shows the higher reaction reactivity and the formation temperatures of most cycloalkenes and aromatics are lower than those in the *m*-xylene pyrolysis. Such differences can be explained by the lower BDEs of methyl scission (R1) on 3-ethyltoluene leading to the decomposition of the fuel and formation of products at lower temperatures. The formation pathways of 1,3-cyclopentadiene are almost identical between the kinetics of 3-ethyltoluene and *m*-xylene, and so are those of 1,3-cyclohexadiene. Therefore, the concentration shapes of 1,3-cyclopentadiene and 1,3-cyclohexadiene in Fig. 6a and b suggest that the different formation behaviors mainly depend on their primary fuel reactivities.

The primary fuel decomposition behaviors also influence the formations of benzene, naphthalene and methylindene isomers, because their formations require the participation of *m*-methylbenzyl radicals. Different from successive hydrogen scissions in naphthene pyrolysis [18,19] for benzene formation, abundant benzene is produced by the decomposition of 3-methylfulvenallene, which is evolved from the *m*-methylbenzyl radical [16] in the pyrolysis of 3-ethyltoluene. The formation of naphthalene is governed by the combination of *m*-methylbenzyl and acetylene in the Battin-Leclerc's model [7]. However, this formation pathway has been changed to *o*-methylbenzyl + C_2H_2 → naphthalene in the present work considering the adjacent carbon skeleton of naphthalene. For the four methylindene isomers in Fig. 6f, 4-methylindene is deemed to be the most likely one which is significantly affected by the formations of the *m*-methylbenzyl and acetylene. Compared with naphthalene, the formation temperatures of 4-methylindene are at least 50 K lower than those of naphthalene and the isomerization from *m*- to *o*-methylbenzyl exactly provides the reasonable explanation for the gap of the temperature window.

Another important feature for the 3-ethyltoluene pyrolysis is that the ethyl substituent bonded to benzene ring results in the easy formation of toluene, stilbene and bibenzyl. The ethyl group can be replaced by a hydrogen atom, producing toluene and corresponding ethyl radical. Due to the relatively lower BDE of ethyl scission than that of methyl scission in *m*-xylene, the contribution to the toluene production increases distinctly under the pyrolysis of 3-ethyltoluene. In addition, the reaction 3-ethyltoluene + H → toluene + ethyl is a one-step fuel decomposition reaction leading to more than 52 K temperature gap between the formation points for benzene and toluene (Fig. 6c and d). The formation routes for stilbene and bibenzyl are originally from the combination of two benzyl radicals, which are generally formed by hydrogen abstraction from toluene in the *m*-xylene pyrolysis. In the 3-ethyltoluene pyrolysis, the yield of benzyl radical is promoted benefited from ethylbenzene decomposition [2]. Connections between stilbene and bibenzyl are the two steps of hydrogen elimination from the secondary carbon atoms between two phenyl groups.

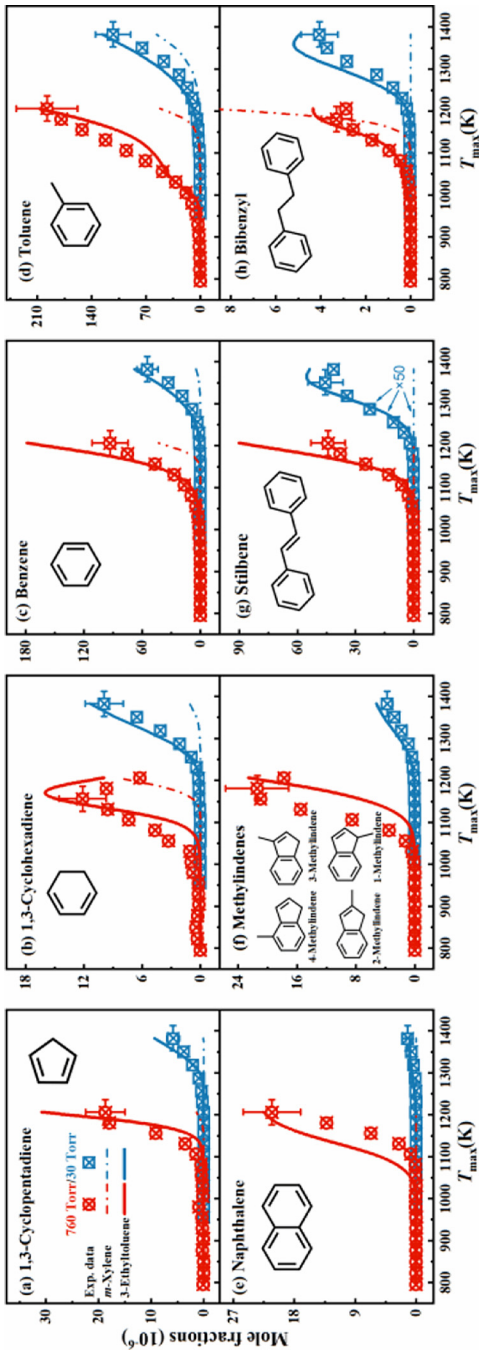

Fig. 6. Measured (symbols) and simulated (lines) concentration profiles of cycloalkenes and aromatics in the pyrolysis of 3-ethyltoluene.

5. Conclusions

High temperature pyrolysis of 3-ethyltoluene under low and atmospheric pressures was investigated in this work with insights into model implications based on quantitative speciation information of fuel-specific intermediates. Over thirty intermediates were detected and determined with the assistance of synchrotron VUV-PI-MBMS. A kinetic model of 3-ethyltoluene was developed. Methyl-dissociated reaction from ethyl group of 3-ethyltoluene with relatively low BDE is found to be the dominant pathway for the fuel consumption, and hydrogen abstractions from methyl and ethyl substitutes also play the vital role in the fuel decomposition. Direct observations of ortho and para methylbenzyl radicals, together with the ortho and para xylylenes under pyrolysis conditions verify the derivation of the isomerization and decomposition of methylbenzyl isomers in the previous theoretical calculations. Implications for reaction mechanism on rearrangements of *o*-xylylene were proved by the experimental detection of styrene and benzocyclobutene, which further confirm the matter that *m*-methylbenzyl can transform to neighboring *o*-methylbenzyl radical. Several observed ethylbenzyl radicals and indane undertake the key joints in the reaction pattern for their formation and consumption pathways. Effects of the fuel structural features on the pyrolysis behaviors are highlighted in this work by comparing the 3-ethyltoluene with *m*-xylene on the performances of cycloalkenes and aromatics predictions. The ethyl group in 3-ethyltoluene improves the reaction reactivity, which boosts the reaction process to facilitate the production of cycloalkenes and promote the formation of aromatics and PAHs.

Declaration of Competing Interest

The authors declare that they have no known competing financial interests or personal relationships that could have appeared to influence the work reported in this paper.

The authors declare the following financial interests/personal relationships which may be considered as potential competing interests:

Acknowledgements

Authors are grateful for the funding support from the National Natural Science Foundation of China granted for U2032119, 71690245 and 51706217.

Supplementary materials

Supplementary material associated with this article can be found, in the online version, at doi:10.1016/j.proci.2022.07.150.

References

[1] W. Sun, A. Hamadi, S. Abid, N. Chaumeix, A. Comandini, A comparative kinetic study of C8–C10 linear alkylbenzenes pyrolysis in a single-pulse shock tube, Combust. Flame 221 (2020) 136–149.

[2] W. Yuan, Y. Li, G. Pengloan, C. Togbé, P. Dagaut, F. Qi, A comprehensive experimental and kinetic modeling study of ethylbenzene combustion, Combust. Flame 166 (2016) 255–265.

[3] K. Hemelsoet, V. Van Speybroeck, M. Waroquier, A DFT-based investigation of hydrogen abstraction reactions from methylated polycyclic aromatic hydrocarbons, ChemPhysChem 9 (2008) 2349–2358.

[4] C. Ji, E. Dames, H. Wang, F.N. Egolfopoulos, Propagation and extinction of benzene and alkylated benzene flames, Combust. Flame 159 (2012) 1070–1081.

[5] D. Han, S. Deng, W. Liang, P. Zhao, F. Wu, Z. Huang, C.K. Law, Laminar flame propagation and nonpremixed stagnation ignition of toluene and xylenes, Proc. Combust. Inst. 36 (2017) 479–489.

[6] H.-P.S. Shen, M.A. Oehlschlaeger, The autoignition of C8H10 aromatics at moderate temperatures and elevated pressures, Combust. Flame 156 (2009) 1053–1062.

[7] F. Battin-Leclerc, R. Bounaceur, N. Belmekki, P.A. Glaude, Experimental and modeling study of the oxidation of xylenes, Int. J. Chem. Kinet. 38 (2006) 284–302.

[8] S. GaÏL, P. Dagaut, Oxidation of m-xylene in a JSR: experimental study and detailed chemical kinetic modeling, Combust. Sci. Technol. 179 (2007) 813–844.

[9] S. Gudiyella, T. Malewicki, A. Comandini, K. Brezinsky, High pressure study of m-xylene oxidation, Combust. Flame 158 (2011) 687–704.

[10] L. Zhao, Z. Cheng, L. Ye, F. Zhang, L. Zhang, F. Qi, Y. Li, Experimental and kinetic modeling study of premixed o-xylene flames, Proc. Combust. Inst. 35 (2015) 1745–1752.

[11] T. Bierkandt, P. Hemberger, P. Oßwald, M. Köhler, T. Kasper, Insights in m-xylene decomposition under fuel-rich conditions by imaging photoelectron photoion coincidence spectroscopy, Proc. Combust. Inst. 36 (2017) 1223–1232.

[12] A. Roubaud, O. Lemaire, R. Minetti, L.R. Sochet, High pressure auto-ignition and oxidation mechanisms of o-xylene, o-ethyltoluene, and n-butylbenzene between 600 and 900 K, Combust. Flame 123 (2000) 561–571.

[13] B.L. Smith, T.J. Bruno, Composition-explicit distillation curves of aviation fuel JP-8 and a coal-based jet fuel, Energy Fuels 21 (2007) 2853–2862.

[14] P. Hemberger, A.J. Trevitt, E. Ross, G. da Silva, Direct observation of para-xylylene as the decomposition product of the meta-xylyl radical using VUV synchrotron radiation, J. Phys. Chem. Lett. 4 (2013) 2546–2550.

[15] P. Hemberger, A.J. Trevitt, T. Gerber, E. Ross, G. da Silva, Isomer-specific product detection of gas-phase xylyl radical rearrangement and decomposition using VUV synchrotron photoionization, J. Phys. Chem. A 118 (2014) 3593–3604.

[16] G. da Silva, E.E. Moore, J.W. Bozzelli, Decomposition of methylbenzyl radicals in the pyrolysis and oxidation of xylenes, J. Phys. Chem. A 113 (2009) 10264–10278.

[17] F. Qi, Combustion chemistry probed by synchrotron VUV photoionization mass spectrometry, Proc. Combust. Inst. 34 (2013) 33–63.

[18] Q. Wang, C. Wang, Y. Huang, M. Ding, J. Wang, J. Yang, Pyrolysis chemistry of n-propylcyclohexane via experimental and modeling approaches, Fuel 283 (2021) 118847.

[19] Q. Wang, C. Wang, Y. Huang, M. Ding, J. Yang, J. Wang, A kinetic study on pyrolysis of iso-propylcyclohexane: Fuel structure effects of alkylcyclohexane isomers on reaction mechanisms, Proc. Combust. Inst. 38 (2021) 489–497.

[20] A.G. Mouis, A. Menon, V. Katta, T.A. Litzinger, M. Linevsky, R.J. Santoro, S.P. Zeppieri, M.B. Colket, W.M. Roquemore, Effects of m-xylene on aromatics and soot in laminar, N2-diluted ethylene co-flow diffusion flames from 1 to 5atm, Combust. Flame 159 (2012) 3168–3178.

[21] G. Kukkadapu, D. Kang, S.W. Wagnon, K. Zhang, M. Mehl, M. Monge-Palacios, H. Wang, S.S. Goldsborough, C.K. Westbrook, W.J. Pitz, Kinetic modeling study of surrogate components for gasoline, jet and diesel fuels: C7-C11 methylated aromatics, Proc. Combust. Inst. 37 (2019) 521–529.

[22] L.J. Mizerka, J.H. Kiefer, The high temperature pyrolysis of ethylbenzene: evidence for dissociation to benzyl and methyl radicals, Int. J. Chem. Kinet. 18 (1986) 363–378.

[23] A. Ergut, S. Granata, J. Jordan, J. Carlson, J.B. Howard, H. Richter, Y.A. Levendis, PAH formation in one-dimensional premixed fuel-rich atmospheric pressure ethylbenzene and ethyl alcohol flames, Combust. Flame 144 (2006) 757–772.

[24] T.A. Litzinger, K. Brezinsky, I. Glassman, The oxidation of ethylbenzene near 1060K, Combust. Flame 63 (1986) 251–267.

[25] I.D. Costa, R. Fournet, F. Billaud, F. Battin-Leclerc, Experimental and modeling study of the oxidation of benzene, Int. J. Chem. Kinet. 35 (2003) 503–524.

[26] W. Yuan, L. Zhao, S. Gaïl, J. Yang, Y. Li, F. Qi, P. Dagaut, Exploring pyrolysis and oxidation chemistry of o-xylene at various pressures with special concerns on PAH formation, Combust. Flame 228 (2021) 351–363.

[27] R.X. Fernandes, A. Gebert, H. Hippler, The pyrolysis of 2-, 3-, and 4-methylbenzyl radicals behind shock waves, Proc. Combust. Inst. 29 (2002) 1337–1343.

[28] Y. Zhang, X. Zhang, C. Cao, J. Zou, T. Li, J. Yang, L. Ye, Y. Li, Flow reactor pyrolysis of iso-butylbenzene and tert-butylbenzene at various pressures: Insight into fuel isomeric effects on pyrolysis chemistry of butylbenzenes, Proc. Combust. Inst. 38 (2021) 1423–1432.